# AIAA 2006-7126

# Solid Modeling of Crew Exploration Vehicle Structure Concepts for Mass Optimization

**V. Mukhopadhyay**
**NASA Langley Research Center, Hampton, VA**

**11th AIAA/ISSMO Multidisciplinary Analysis and Optimization Conference**
**6-8 September 2006**
**Portsmouth, VA**

AIAA 2006-7126

# Solid Modeling of Crew Exploration Vehicle Structure Concepts for Mass Optimization

Vivek Mukhopadhyay*
*NASA Langley Research Center, Hampton, VA*

**Parametric solid and surface models of the crew exploration vehicle (CEV) command module (CM) structure concepts are developed for rapid finite element analyses, structural sizing and estimation of optimal structural mass. The effects of the structural configuration and critical design parameters on the stress distribution are visualized, examined to arrive at an efficient design. The CM structural components consisted of the outer heat shield, inner pressurized crew cabin, ring bulkhead and spars. For this study only the internal cabin pressure load case is considered. Component stress, deflection, margins of safety and mass are used as design goodness criteria. The design scenario is explored by changing the component thickness parameters and materials until an acceptable design is achieved. Aluminum alloy, titanium alloy and an advanced composite material properties are considered for the stress analysis and the results are compared as a part of lessons learned and to build up a structural component sizing knowledge base for the future CEV technology support. This independent structural analysis and the design scenario based optimization process may also facilitate better CM structural definition and rapid prototyping.**

## I. Introduction

Mass estimation of aerospace vehicles requires significant experience and extrapolation of available data from previously developed vehicles[1,2]. In this paper, a physics based approach is used, in order to explore the design alternatives. First, several parametric solid and surface models are developed for visualization of vehicle configuration options, structural sizing and mass estimation through finite element analysis. Previously, solid models of a simple conical uniform shell, spar, ring and double skin ribbed shell and isogrid panel constructions were investigated[3] in order to examine their effects on the stress distribution, deflection, margins of safety and structural mass. In this study, refined and improved solid and surface models are presented. The results from this physics based analysis and design approach are presented as a part of lessons learned and to build up a structural sizing knowledge base for future technology support. However, these structural analysis results were highly conceptual and exploratory in nature and do not reflect the current configuration designs being conducted at the program level by NASA and the aerospace industry.

*Senior Research Engineer, Aeronautical Systems Analysis Branch /ms442, Associate fellow, AIAA.

The paper is organized as follows. The baseline vehicle as defined in the Exploration Systems Architecture Study[1] is reviewed first, followed by a review of the Apollo command module structural configuration. Then developments of the command module solid and surface models are described. The solid and surface model finite element analyses results are compared. The surface model is analyzed further, with several sets of shell thicknesses and materials, in order to explore the design scenario and build up the knowledge base. The initial results are presented in tabular and graphical form for initial comparison of the design options.

## II. Baseline Structure

In the NASA's Exploration Systems Architecture Study[1] (ESAS), a set of conceptual design of the Crew Exploration Vehicle (CEV) were presented. The CEV Command Module configuration consisted of the Command Module (CM), Crew Service Module (CSM) and the Launch Abort System (LAS). The CM structure configuration was defined as the outer thermal protection shield, and the crew cabin with windows and hatches. The selected outer mold line (OML) for the CM is similar to the Apollo Command Module shape

scaled in dimension by approximately 141 percent to a base diameter of 5.5 m (18 ft), while the original Apollo Command Module sidewall angle of 32.5 deg has been maintained for this analysis. Selecting this shape provides a total CEV pressurized volume of 29.4 $m^3$ (1,038 $ft^1$). The CEV pressure vessel structure provides habitable volume for the crew and enclosure for necessary systems of the CEV through ascent until rendezvous with the Lunar Surface Access Module (LSAM) in low Earth orbit, through transit to the Moon and transfer to the LSAM in lunar orbit, and through undocking from the LSAM in lunar orbit until reentry and crew recovery on Earth.

In the ESAS study report[1], the CEV Command Module pressurized cabin structure construction was an Aluminum (AL) honeycomb sandwich using materials such as AL2024 or the equivalent for the face sheets and AL5052 for the honeycomb core. The mass-estimating method used for estimating pressure vessel structure (including secondary structure) in this assessment was to assume a uniform structure mass per unit area and scale by the external surface area of the pressure vessel. The assumed scaling factor for aluminum honeycomb is 20.3 $kg/m^2$ (4.15 $lb/ft^2$) and the surface area of the pressure vessel without the windows and hatches is 52.7 $m^2$.

The pressure vessel structure mass for the CM was designed to withstand a higher 1.0139E+5 $N/m^2$ (14.7 psi) nominal internal cabin pressure required for the International Space Station (ISS) crew rotation missions instead of the lower 9.5 psi nominal internal pressure for lunar missions. The Apollo CM had mass of approximately 5,800 kgm with a structure mass component of 1570 kgm, or a mass fraction of 0.27. The four crew lunar mission CM mass was estimated to be approximately 9500 kg, and the structural mass is assumed as 2777 kgm including structure and thermal protection. This CM mass constitutes a mass fraction of 0.29 of the total CM mass. The structural mass part without the heat shield was estimated at about 1883 kgm.

## III. Apollo CM Structure

Figure 1 shows the Apollo Command Module capsule. The Command Module was a truncated cone measuring 10 feet 7 inches (3.2 m) tall and having a diameter of 12 feet 10 inches (3.9 m) across the base. The forward compartment contained two reaction control engines, the docking tunnel, and the components of the Earth Landing System (ELS). The inner pressure vessel housed the crew accommodations, equipment bays, controls and displays, and many spacecraft systems. The last section, the aft compartment, contained 10 reaction control engines and their related propellant tanks, fresh water tanks, and the CSM umbilical cables.

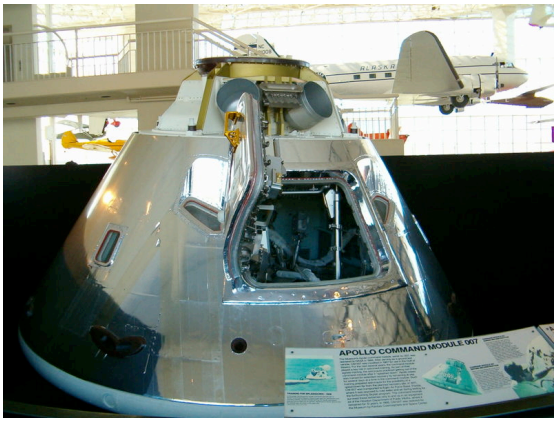

Figure 1. Apollo Command Module.

Construction: The command module's inner structure was an aluminum "sandwich" consisting of a welded aluminum inner skin, a thermally bonded honeycomb core, and a thin aluminum "face sheet". The central heat shield consisted of 40 individual panels interspersed with several holes and openings for the reaction control engines and after-compartment equipment access. The central compartment structure consisted of an inner aluminum face sheet with a steel honeycomb core, a glass-phenolic ablative honeycomb heat shield, a layer of q-felt fibrous insulation, a pore seal, a moisture barrier, and a layer of aluminized PET film thermal strips. The aft heat shield consisted of four brazed honeycomb panels, four spot-welded sheet metal fairings, and a circumferential ring. The fairing segments were attached to the honeycomb panels and ring with conventional fasteners. The steel honeycomb core and outer face sheets were then thermally bonded to the inner skin in a giant autoclave. The aft heat shield is nearly identical to the central, with the exception of the outer aluminized PET film layer. The components of the earth Landing System (ELS) were housed around the forward docking tunnel. The forward compartment was separated from the central by a bulkhead and was divided into four 90-degree wedges.

Hatches: The forward docking hatch was mounted at the top of the docking tunnel. It was 30 inches (760 mm) in diameter and weighed 80 pounds (36 kg). It was constructed from two machined rings that were weld-joined to a brazed honeycomb panel. The exterior side was covered with half-inch (12.7 mm) thick insulation and a layer of aluminum

foil. It was latched in six places and operated by a pump handle. At the center was a pressure equalization valve, used to equalize the pressure in the tunnel and lunar module before the hatch was removed. The Unified Crew Hatch (UCH) measured 29 inches (737 mm) high, 34 inches (864 mm) wide, and weighed 225 pounds (102 kg). It was operated by a pump handle, which drove a ratchet mechanism to open or close 15 latches simultaneously.

Cabin Interior: The central pressure vessel of the command module was its sole habitable compartment. It had an interior volume of 210 cubic feet (5.9 $m^3$) and housed the main control panels, crew seats, guidance and navigation systems, food and equipment lockers, the waste management system, and the docking tunnel. The three crew couches were constructed from hollow steel tubing and covered in a heavy, fireproof cloth. The couches rested on eight shock attenuation struts to ease the impact of splashdown.

## IV. Assumptions and Procedures

In the NASA Procedural Requirement document NPR 8705.2, the minimum factor of safety for manned mission vehicles is specified to be 2.0. The NPR 8705.2 also specified a 1.5 factor of safety on burst pressure for fluid pressure vessels; a 1.4 ultimate factor of safety on all new or redesigned structures; and a 1.25 factor of safety on proof pressure for fluid pressure vessels. In addition to the internal pressure load, this CEV must withstand ballistic inertia lift up load up to 15g during emergency launch abort, external peak temperature of 3000 deg Kelvin thermal load during renter, 16 g landing load, a maximum assent dynamic pressure of about 800 pounds per square foot at a Thrust/Weight ratio of 0.3. In order to carry this extreme mission load in this conical shaped capsule without significant structural mass penalty,[4,5] extensive structural analyses, design, optimization along with the fabrication and testing efforts would be required. With the current structural technology and design tools, there is opportunity for developing significantly efficient structural configurations for these vehicles. The initial assumptions for overall sizing and loads are as follows.

1. The CEV maximum outer diameter is 5.5 meters (216.5 inch).
2. The CM internal cabin design pressure is 101.3 KPascals (14.7 psi) with a factor of safety of 2 for human rated mission.
3. Aluminum alloy AL7050-T73651, Titanium alloy Ti4Al6V, Stitched Advanced Composite Technology Resin Film Injection (ACT-RFI) material are considered. Thermal effects or external loads are not included at this stage.

## V. Solid and Surface Model Development

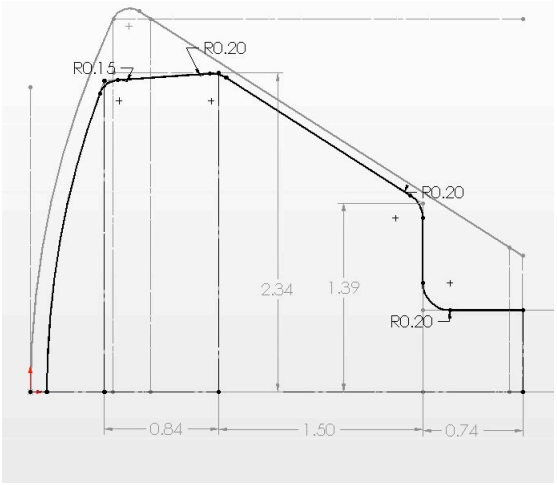


Figure 2. A notional CEV command module section drawing.

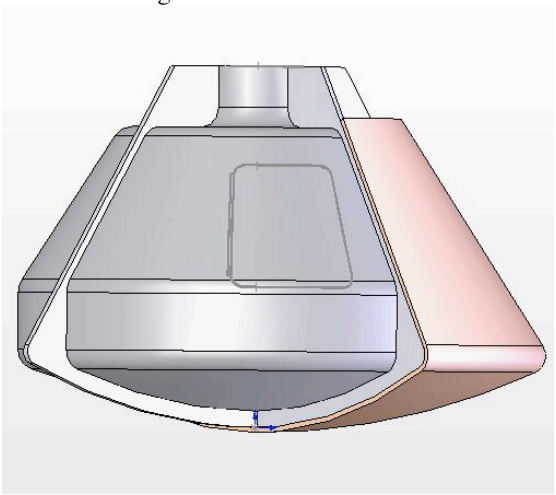

Figure 3. CM capsule solid model cutout view with inner and outer shell, and ribs.

A basic cross section of the CM used for the solid and surface model development is shown in Figure 2. All the independent dimension parameters are shown in this cross section drawing. These dimension parameters can be changed to build and analyze derivative configurations. In the solid and surface models derived from this basic cross section, the inner and outer shell skin thicknesses are used as primary design parameters. A commercial solid modeling tool was used for developing this parametric solid model as well as subsequent surface model. Additional plug-in tools are used for solid and surface meshing, adding

loads, boundary conditions and computing the stress, deflection, mass, moment of inertia, center of gravity location, etc. This tool can also be used for creating engineering drawing for prototype development.

The solid and surface models developed are shown in Figures 3-5. These models were developed and progressively modified for improvement. The parametric solid and surface models were developed based on the section geometry shown in Figure 2. These models were refined from those presented in Ref. 3 with 0.15 to 0.2 meter diameter fairing at all the corners of the inside and outer shell. Figure 3 shows the CM capsule solid model cutout view with inner and outer shell, and 4 ribs at 90 degrees interval.

The solid model in shown in Figure 4 has an inner shell of 7 mm thickness. The outer shell represents the heat shield. The 70 mm gap between the inner and outer shell is filled with thermal insulation, q-felt and moisture barrier. Eight spars were initially modeled and spaced at 45 degrees interval. Each spar is modeled with 7 mm thick AL7050 plate. The exit tunnel is supported by 4 wedges at 90 degrees interval. These wedges and spars support and transfer the impulsive thrust if the launch abort rocket is activated.

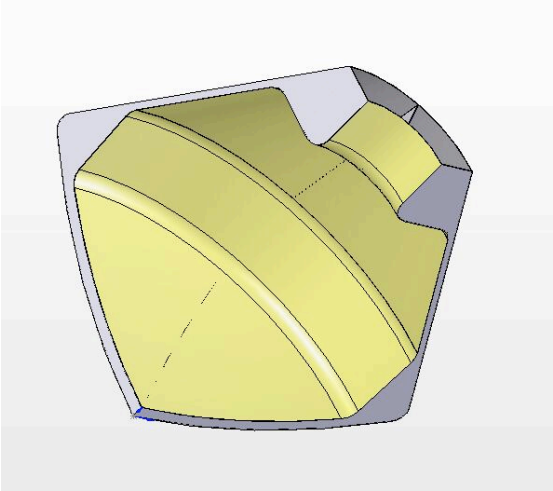

Figure 4. Quad CM solid model (CEV5d)

The structural finite element analysis process steps are as follows.

1. Generate parametric solid models of the vehicle outer shell, and pressurized tank components.
2. Analyze solid and shell finite element models (FEM) of vehicle components and compute stress, deflection and safety margins, based on the internal pressure load.
3. Resize solid or shell models, choose materials and skin thickness that would meet or exceed the specified margins of safety based on the material yield stress.
4. Conduce a design scenario with a series of thicknesses and material and how summary of data and results in Tables.
6. Modify FEM models for additional structural analysis with all external loads, for sizing, stability and optimization studies.

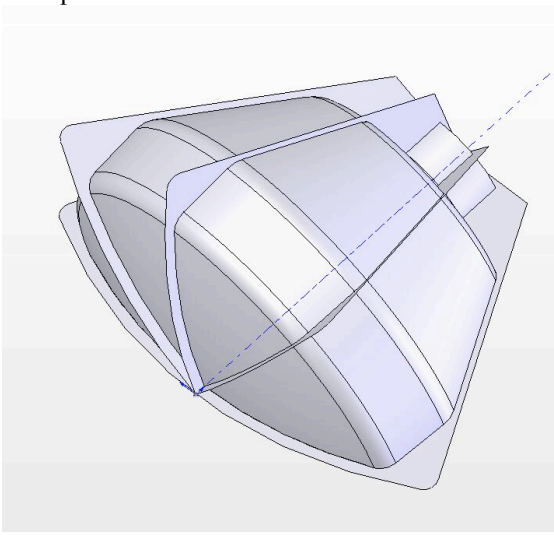

Figure 5. Half CM surface model without the outer shell and 8 spars (CEV6b).

## VI. Inner and Outer shell Solid Model (CEV5d-solid7)

For the command module shell analysis, high strength Aluminum AL7050-T73651 alloy is used. This aluminum alloy has high fracture toughness. Additional results using Titanium alloy material properties are also presented for comparison. The material properties[6] used for this analysis are shown in Table 2. The solid and surface models are developed using SolidWorks[7], commercial CAD software. The finite element model stress analysis was performed using CosmosDesignStar[8] for both solid and shell models. First a solid model of the conical inner and outer shell with internal ribs and ring bulkheads in between the inner and outer shell were developed and analyzed. These preliminary analysis results were presented in Ref. 3. Only an internal pressure load of 101.3 KPascals (14.7 psi: pounds per square inch) was used for these analyses.

The first quadrant of the inner pressurized shell without cutouts was modeled as shown in Figure 4. The FEM analysis was done with a dense mesh containing 250000 tetrahedral 3D elements.

A fixed boundary condition was imposed on the heat shield outer edge along the maximum diameter. Symmetric boundary conditions are imposed on the ribs which form the boundary symmetry plane of this quarter model. The von-Mises stress distribution on the top surface of the shell element nodes are shown in Figure 6. From this finite element analysis, the maximum von Mises nodal stress was 1.49E+08 $N/m^2$ (21600 psi), at the edge fillet near the maximum diameter and at the spar and shell junctions.

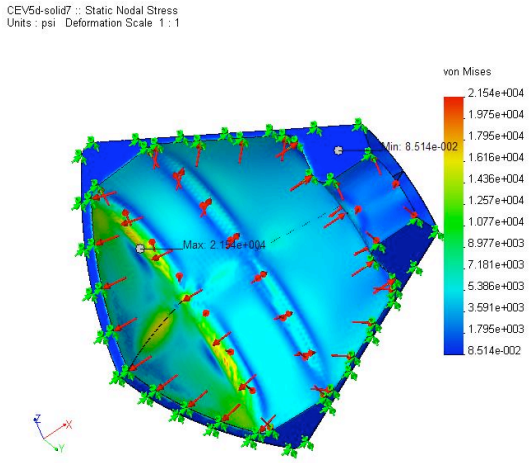


Figure 6. Von-Mises Stress distribution due to the 1.0139E+5 $N/m^2$ (14.7 psi) normal internal pressure distributions (solid model CEV5d).

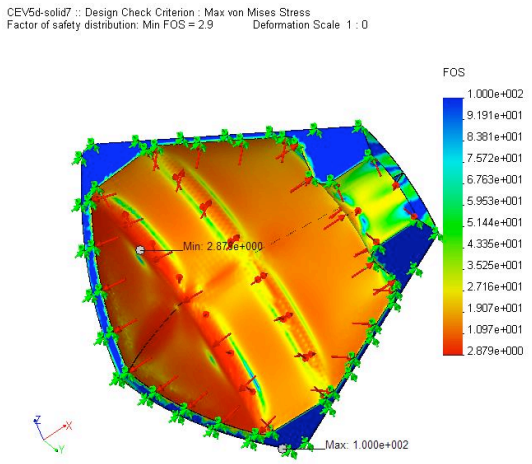


Figure 7. The ratio of Yield Stress/von-Mises stress distribution due to 14.7 psi cabin pressure.

The ratio of Yield Stress/von-Mises stress on the top surface of the shell element nodes is shown in Figure 7. The minimum ratio is 2.9 for this boundary condition. The location is at the mid point between the spars near the corner fairing at the maximum diameter location. Significant structural weight saving may be achieved by reinforcing these areas and reducing the skin thicknesses in other areas which exhibit much higher margins of safety. The maximum deflection under this boundary condition is 0.35 inches. The finite element model mass of the complete capsule is computed to be 2616 kgm mass (4*654 kgm or 5767 pounds).

## VII. Inner and outer shell Surface Model (CEV6b-shell7)

These finite element results from the solid models require solutions close to a quarter million tetrahedral elements and near a million degrees of freedom. Although the inner and outer shell fairings are modeled in precise details, the spar and shell junctions were not filleted and usually would exhibit higher local stresses. The FEM analysis computations of solid models may take up 10 minutes of clock time. In order to quickly perform a large number of parametric studies with shell thicknesses as design parameters, a surface model is often convenient. However the initial surface model may take longer time to develop in order to maintain surface compatibility and continuity. Hence a number of solid and surface models were developed using the same topology, for comparison purposes. The computation clock time for the FEM analysis of this surface model is a few seconds compared to that of the solid FEM model which takes a few minute. The stress and deflection results from identical solid and surface models were generally found to be comparable. The differences were less that 5% percent. Thus the surface models were more suited for a parametric analysis and optimization study.

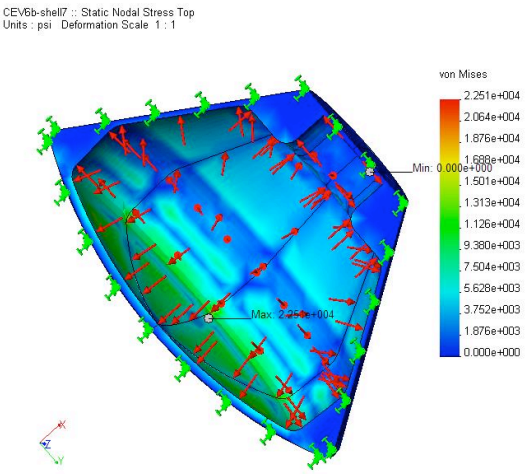


Figure 8. Von-Mises Stress distribution due to the 1.0139E+5 $N/m^2$ (14.7 psi) internal cabin pressure (surface model CEV6b)

The results of the finite element analysis with the same material and loads using the surface model of half the CM capsule (CEV6b-Figure 5) are shown in Figures 8 and 9. In this case the boundary condition is imposed by fixing the two diametrically opposite spar frame. The von-Mises stress distribution shown in Figures 8 indicates a maximum von-Mises stress of 1.56E+08 N/m$^2$ (22560 psi).

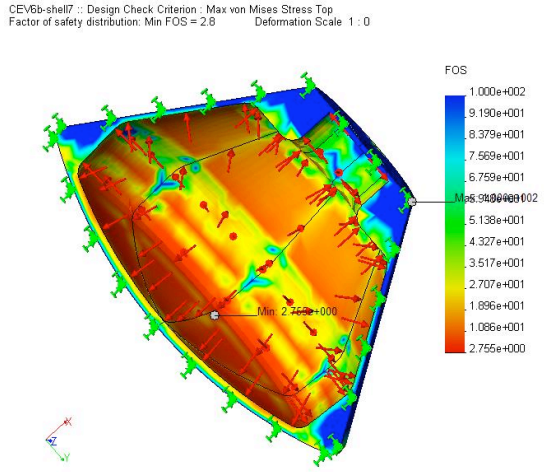


Figure 9. The ratio of Yield Stress/von-Mises stress distribution due to the 1.0139E+5 N/m$^2$ (14.7 psi) internal cabin pressure, with minimum margin of safety 2.75.

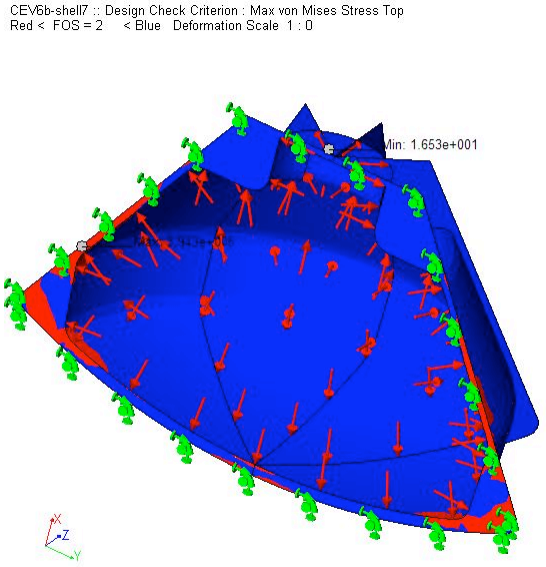


Figure 10. The ratio of the yield stress/von-Mises stress above 2.0 is shown by the blue region., and below 2.0 by red region (Minimum ratio 0.16).

The Yield stress/von-Mises stress ratio distribution on the top surface, shown in Figure 9 indicates that the minimum ratio of 2.8. By comparing the Figures 6, and 7 with those in Figure 8, and 9 respectively, one may conclude that the solid model and the surface model provide comparable results, although the surface models have only 5600 shell elements. The finite element model mass of the complete capsule is computed to be 2674 kgm mass (2x1337 kgm or 5895 pounds). The slightly higher mass of the surface model is due to the inclusion of the forward cone of the outer shell and the tunnel door hatch wall.

When the FEM analysis is done with the external shell excluded from the structure, the ratio of yield stress/von-Mises stress distribution is as shown in the Figure 10. The blue area indicates region where the ratio is above 2. The minimum ratio is 0.16 locally, but mostly they are above 2.0, as indicated by the blue region. The corresponding mass of the inner shell structure is 1320 (2x660) kg without outer shell.

## VIII. Advanced Composite ACT RFI material Model (CEV6b-shellACT10)

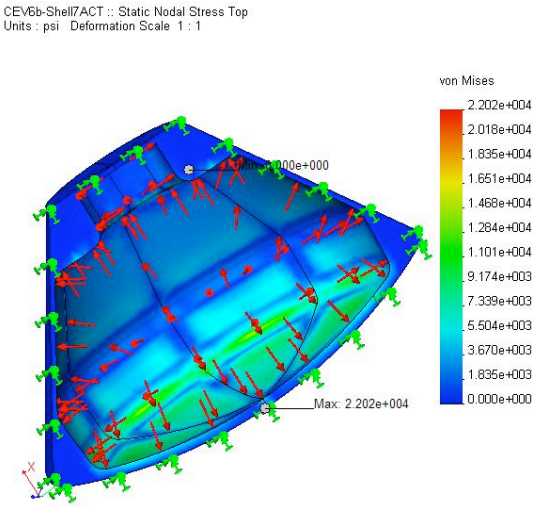


Figure 11. Von-Mises Stress distribution due to the 1.0139E+5 N/m$^2$ (14.7 psi) internal cabin pressure (surface model CEV6bShell7ACT-RFI 10).

The same surface model shown in figures 8 and 9 was analyzed with composite material. This advanced composite technology material is constructed with exact shaped stitched woven carbon fiber cloth which is shape-formed and cured after resin film is injected inside the mold under vacuum. Although this material is generally anisotropic, an isotropic property set was used, as shown in Table 2. The thickness of all the structural components had to be increased from 7mm to 10mm in order to achieve the minimum

factor of safety of 2. The maximum stress was computed to be 1.52E+08 N/meter$^2$ (22000 psi), as shown in Figure 11.

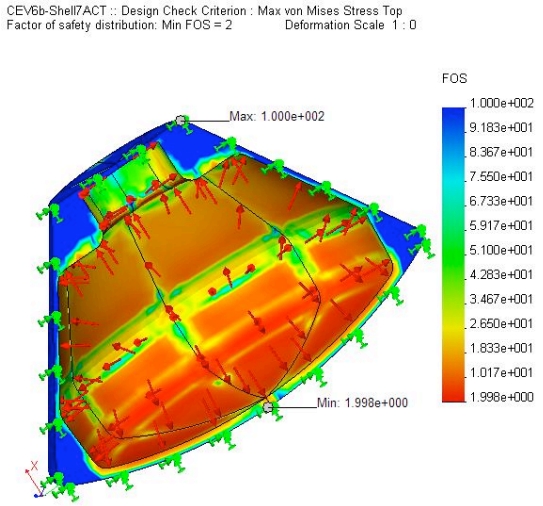


Figure 12. The ratio of Yield Stress/von-Mises stress distribution due to the 14.7 psi internal cabin pressure (surface model CEV6bShell7ACT-RFI 10) with minimum margin of safety 2.0.

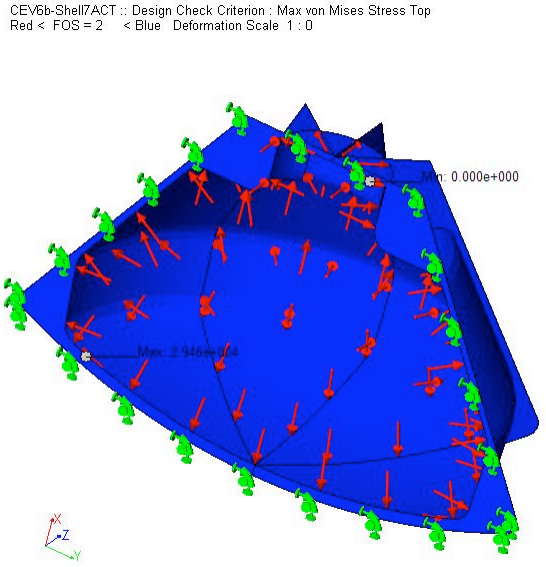


Figure 13. The ratio of the yield stress/von-Mises stress above 2.0 is shown by the blue region, and below 2.0 by red region (Minimum ratio 1.5).

The ratio of Yield Stress/von-Mises stress on the top surface of the shell element nodes is shown in Figure 12. This figure indicates that the ratio is just under 2.0, near the center of the curved shell at the shell-spar junction. The structural mass is about 2232 kgm (2x1116 kgm) which was 442 kgm lower than that obtained from analysis described in the previous section with aluminum AL7050 material. However, concern for using composite materials such as high fabrication cost, health monitoring, maintenance, resin outgassing, delaminating, thermal effects, lower impact resistance, etc. should be considered before space vehicle application is undertaken.

When the FEM analysis is done with the external shell excluded from the structure, the ratio of yield stress/von-Mises stress distribution is as shown in the Figure 13. The blue area indicates region where the ratio is above 2. The minimum ratio is 1.5 locally near the edge of the heat shield junction. The ratios below 2.0 are indicated by the red region. The corresponding mass of the inner shell structure is 1100 (2x550) kg without outer shell.

## IX. Isogrid Panel

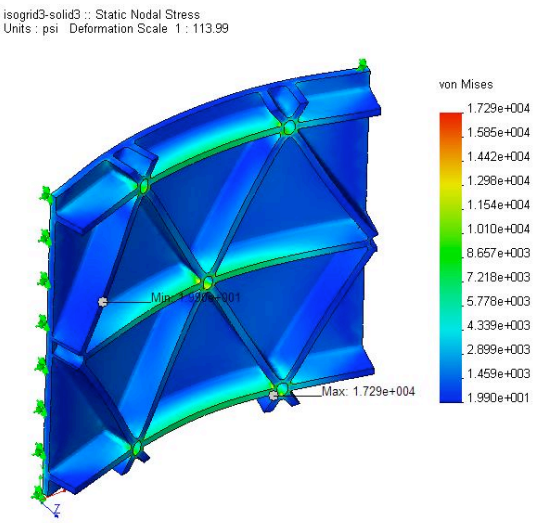


Figure 14. Von-Mises Stress distribution due to the 1.0139E+5 N/m$^2$ (14.7 psi) normal pressure.

For efficient load carrying capacity and mass reduction, isogrid structures are commonly used for launch vehicles. A solid model of an isogrid panel was developed and analyzed. This Isogrid solid model represents a 25.4x25.4 cm (10 inch) square panel, with skin thickness 2.54mm (0.1 inch). The rib thickness of each of the machined isogrid is 5.08mm (0.2 inch). Total skin plus rib height is 25.4 mm (1 inch). The material is AL 7050 alloy. The panel weight is 1.0614 kg, with standard 2.54 mm (0.1 inch) fillet and 1 cm (0.4 inch) diameter drilled holes at each rib

junction. Each side of the isogrid triangle has a length of 12.7 cm (5 inch). With this isogrid panel geometry and material, a panel specific mass per unit panel surface area is estimated as 16.452 kg/m$^2$.

Figure 14 shows von-Mises stress distribution on this isogrid panel due to the uniform 1.0139E+5 N/m$^2$ (14.7 psi) pressure, acting outward. An ideal boundary condition of two opposite outer edge fixed to allow for rotation of the side faces was used. The other two edges are assumed to be free. With this more detailed solid model and the high fidelity finite element analysis with about 20000 solid tetrahedral elements, the maximum local von-Mises stresses occur at the middle of the panel and at the outer edge of the machined ribs and may dominate the design. The maximum von-Mises nodal stress at these locations is 1.192+08 N/m$^2$ (17300 psi). The maximum deflection is 0.22 mm (0.009 inch).

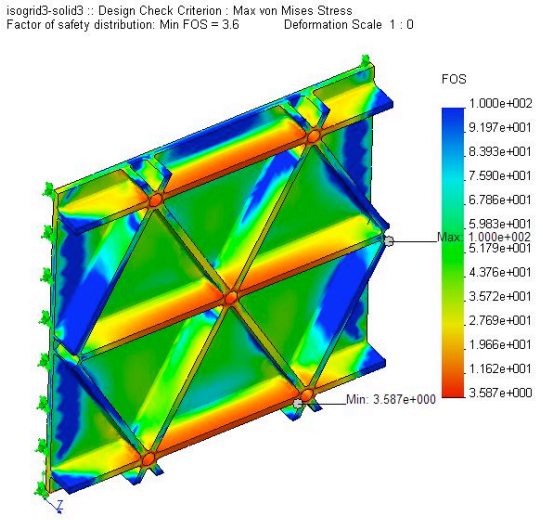


Figure 15. The ratio of Yield Stress/von-Mises stress distribution due to the 1.0139E+5 N/m$^2$ (14.7 psi) normal pressures.

Figure 15 shows the distribution of yield stress/von-Mises stress ratio. The minimum ratio is 3.6 at the edge of the spar and at the hole drilled at the spar-junction. The inner shell of the assumed CM has approximately 60 square meter surface area, including windows and hatches. This would translate into a structural mass of mass of (60x 16.452) 987 kgm with AL7050-T73651 material isogrid skin construction. Thus much higher structural stress factor of safely can be achieved for this higher internal design pressure load, without increasing the structural mass. However for greater accuracy, analytical and empirical buckling analysis of flat and curved cylindrical and spherical segments needs to be performed. An empirical procedure for buckling check and optimization under combined loading is described in Ref. 9.

## X. Conclusions

Structural analysis results of a notional crew exploration vehicle are presented. The effect of the internal cabin pressure load on the stress distribution, margin of safety, mass and deflections are investigated. A design scenario based optimization study was presented, using a) uniform 5 mm, and 7 mm thick skin and spars, with aluminum alloy material; b) 5 mm thick shell skin and spar with titanium alloy material; c) 10 mm thick skin and spars, with advanced composite material, and d) an isogrid skin panel configuration option. The results are summarized in Table 1 and as bar charts in Figures 16 and 17.

A solid quad model and corresponding surface half model were analyzed for initial comparison and validation of the results from the two models. This was to ensure that both the design provide results within 5% of each other. In order to examine the effect of high local stress regions on the design at the skin-spar junctions which were not filleted, an identical quad solid model with 5mm fillet at the skin-spar junction was also analyzed. This reduced the minimum ratio of the yield stress/von-Mises stress from 2.8 to 2.3 or an 18% reduction in local stress with about 25000 solid tetrahedral elements.

With the AL7050 alloy material, the baseline skin thickness of 7 mm was found to be adequate in order to provide a minimum margin of safety of 2.8 for internal pressure. The baseline mass was approximately 2775 kgm including the inner and the outer shell (density 2700 kgm/m3).

With advanced composite material ACT-RFI-MD90 construction, it was necessary to increase the skin and spar thicknesses from 7mm to 10mm in order to provide a minimum margin of safety of 2.0. The corresponding mass was estimated at 2232 kgm including the inner and outer shell (material density 1603 kgm/cubic meters). This represents a mass reduction of 543 kgm.

The external shell represents the shield, and is made of carbon-graphite-phenolic compound impregnated in metal honeycomb. It is designed to withstand reentry thermal and aerodynamic loads.

Since only pressure load is considered for this paper, a second set of analysis was performed with the inner shell only.

With the Ti6Al4V titanium alloy material (density 4556 kgm/m3), the baseline skin thickness of 5 mm was found to be adequate in order to provide a minimum margin of safety of 2.8 for internal pressure load. The inner shell mass was estimated to be approximately 1564 kgm.

With the 7mm thick AL7050 inner shell analysis, the minimum margin of safety for internal pressure load was above 2.0 for most of the shell, except for the edges as shown in Figure 10. The inner shell mass was estimated to be approximately 1320 kgm. This represents inner shell mass reduction of 244 kgm from the titanium inner shell.

With the 10mm thick ACT_RFI MD90 inner shell analysis, the minimum margin of safety for internal pressure load was above 2.0 for most of the shell, except for the edges as shown in Figure 13. The inner shell mass was estimated to be approximately 1100 kgm. This represents inner shell mass reduction of 200 kgm from the aluminum inner shell.

Furthermore, with the isogrid panel construction, inner shell mass is estimated to be 987 kgm, for a 60 square meter surface area. Although this analysis used simplified boundary condition and only pressure loading, the isogrid AL7050 construction appears to provide significant strength/weight ratio with adequate safety margins. This option as well as the titanium alloy materials should be should be investigated farther with full vehicle model. Titanium alloy construction should also be investigated further since it has less developmental risk than the composite material However, additional sizing and optimization studies with all possible design loads are necessary.

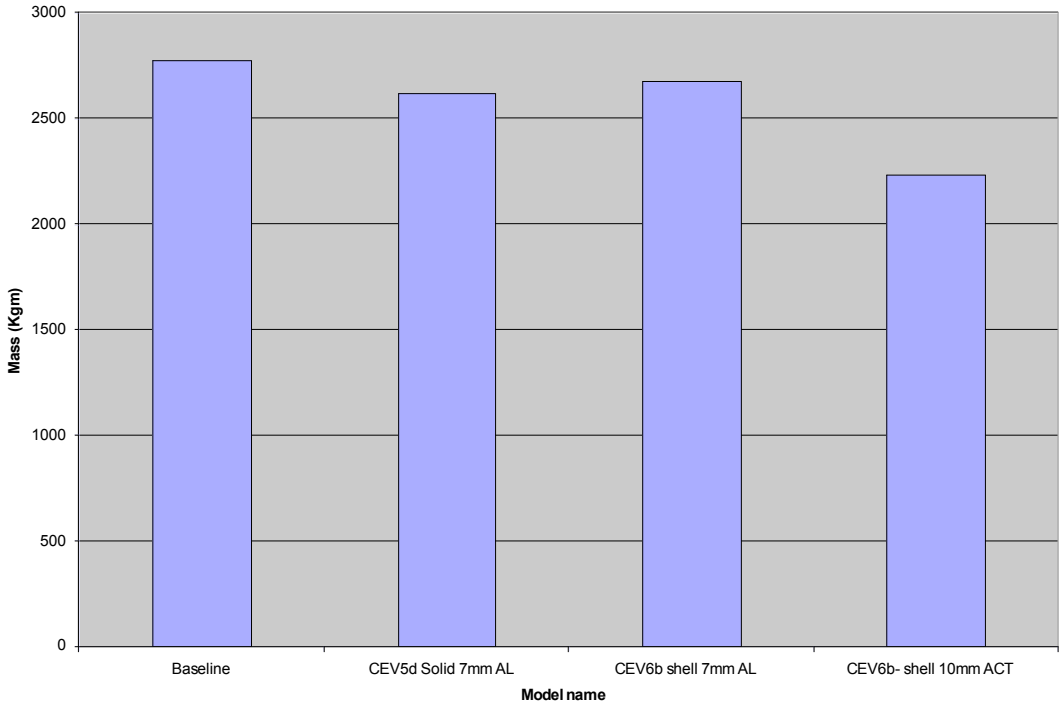


Figure 16. Mass comparison of solid and surface models investigated with Finite element analysis.

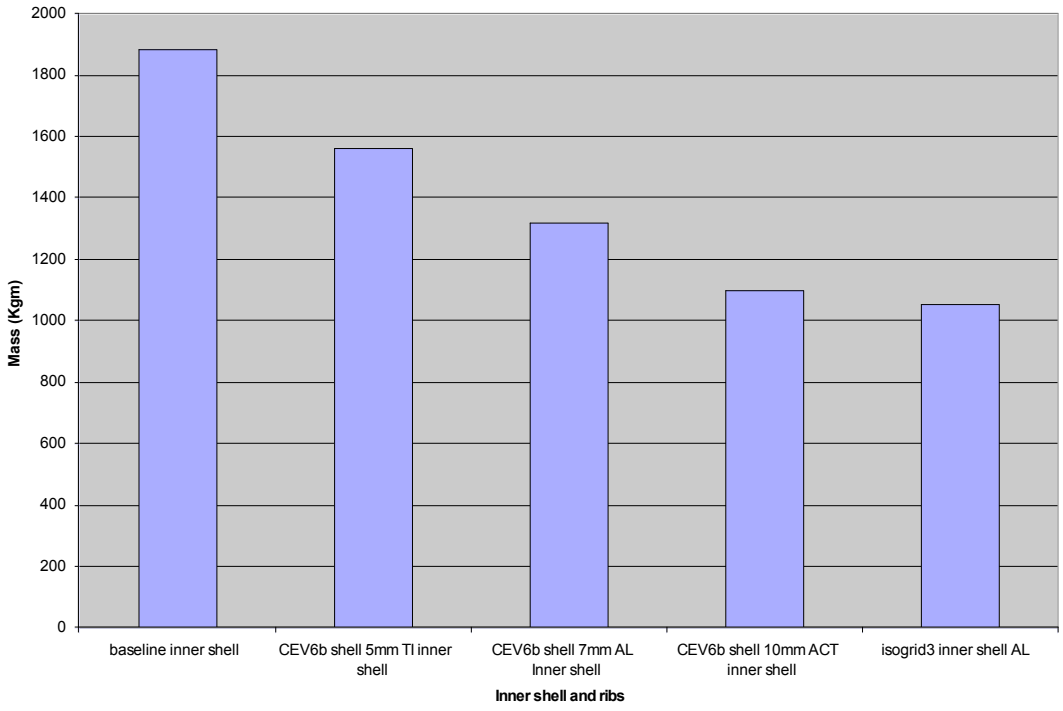


Figure17. Mass comparison of the surface models of CM inner shell and ribs from the Finite element analysis, and sizing with internal pressure loads.

Table 1. Summary results from the set of models analyzed (CEV5, CEV6 and derivatives)

| Model name | model description | pressure load | material | max VM stress psi | N/m2 | min MOS | max defl.mm | mass KGm | Comments |
|---|---|---|---|---|---|---|---|---|---|
| CEV5d Solid 7mm AL | smoother solid model with corner fairing and forward hatch removed, 7mm skin, 8 webs at 45deg interval (quad model) | 101 Kpa (14.7 psi) no end hatch load | AL 7050-T73651 plate | 21600 | 1.49E+08 | 2.9 | 0.35 inches | 2616 | 2616 kg (4x654 kg) inner and outer shell |
| CEV6b shell 7mm AL | smoother surface model with corner fairing, 7mm skin, 8 webs at 45deg interval (half model) | 101 Kpa (14.7 psi) no end hatch load | AL 7050-T73651 plate | 22560 | 1.56E+08 | 2.8 | 12 mm | 2674 | 2674 kg (2x1337 kg) inner and outer shell |
| CEV6b- shell 10mm ACT | smoother surface model with corner fairing, 10 mm skin, 8 webs at 45deg interval (half model) | 101 Kpa (14.7 psi) no end hatch load | ACT_RFI | 22000 | 1.52E+08 | 2 | 10 mm | 2232 | 2232 kg (2x1136 kg) inner and outer shell |
| CEV6b shell 5mm TI inner shell | smoother surface model with corner fairing, 5mm skin, 5 webs at 45deg interval (half model) w/o outer shell | 101 Kpa (14.7 psi) no end hatch load | Ti-6AL4VA | 53180 | 3.67E+08 | 2.8 | 17.5 mm | 1564 | 1564 kg (2x782 kg) inner shell only, mos 2.8 |
| CEV6b shell 7mm AL Inner | smoother surface model with corner fairing, 7mm skin, 8 webs at 45deg interval (half model) w/o outer shell | 101 Kpa (14.7 psi) no end hatch load | AL 7050-T73651 plate | 394300 | 2.72E+09 | 0.16 | 101 mm | 1320 | 1320 kg (2x660 kg) inner shell only, mos |
| CEV6b shell 10mm ACT inner | smoother surface model with corner fairing, 10 mm skin, 8 webs at 45deg interval (half model) w/o outer shell | 101 Kpa (14.7 psi) no end hatch load | ACT_RFI | 29460 | 2.03E+08 | 1.5 | 31 mm | 1100 | 1100 kg (2x550 kg) inner shell only, mos 1.5 |
| isogrid3 inner AL | isogrid panel - 2.5 mm skin 0.5 mm web 25.4 cm skin + web AL7050 2 edge fixed 2 free | 101 Kpa (14.7 psi) | AL 7050-T73651 plate | 17300 | 1.19E+08 | 3.6 | 0.022 mm | 987 | wt 16.452 kg/msq, 987 kg for 60 sqm surface area |

Table 2 Material properties used in the FEM analysis:

| material | type | prop | propsymbol | unit | psi | kgf/cm/cm | N/m2 (Pascals) |
|---|---|---|---|---|---|---|---|
| AL7050-T73651 plate | metal | Ex | EX | | 1.03000E+07 | 7.24174E+05 | 7.10415E+10 |
| | | Nu | NUXY | | 0.33 | | |
| | | G | GXY | | 3.87218E+06 | 2.72246E+05 | 2.67073E+10 |
| | | dens | DENS | lb/cuin | 0.10200 | 0.002823398 | 2823.397773 |
| | | ult ten | SIGXT | | 7.10000E+04 | 4.99188E+03 | 4.89703E+08 |
| | | ult comp | SIGXC | | 6.00000E+04 | 4.21849E+03 | 4.13834E+08 |
| | | sigyield | SIGYLD | | 6.20000E+04 | 4.35910E+03 | 4.27628E+08 |
| | | | | | psi | kgf/cm/cm | N/m2 (Pascals) |
| AL-6061 T651 plate | metal | Ex | EX | | 9.90E+06 | 6.96051E+05 | 6.82826E+10 |
| | | Nu | NUXY | | 0.33 | | |
| | | G | GXY | | 3.72180E+06 | 2.61673E+05 | 2.56701E+10 |
| | | dens | DENS | lb/cuin | 0.098 | 0.002712676 | 2712.676291 |
| | | ult ten | SIGXT | | 4.20000E+04 | 2.95294E+03 | 2.89684E+08 |
| | | ult comp | SIGXC | | 3.50000E+04 | 2.46078E+03 | 2.41403E+08 |
| | | sigyield | SIGYLD | | 3.60000E+04 | 2.53109E+03 | 2.48300E+08 |
| | | | | | psi | kgf/cm/cm | N/m2 (Pascals) |
| Ti6AL4VA plate | metal | Ex | EX | | 16000000 | 1.12493E+06 | 1.10356E+11 |
| | | Nu | NUXY | | 0.33 | | |
| | | G | GXY | | 6.01504E+06 | 4.22906E+05 | 4.14871E+10 |
| | | dens | DENS | lb/cuin | 0.162 | 0.004555968 | 4484.219992 |
| | | ult ten | SIGXT | | 160000 | 1.12493E+04 | 1.10356E+09 |
| | | ult comp | SIGXC | | 145000 | 1.01947E+04 | 1.00010E+09 |
| | | sigyield | SIGYLD | | 150000 | 1.05462E+04 | 1.03458E+09 |
| | | | | | psi | kgf/cm/cm | N/m2 (Pascals) |
| ACT wing laminated mat | composite | Ex | EX | | 9250000 | 6.50350E+05 | 6.37994E+10 |
| ACT-stitched RFI Advanced Composite | | Ey | EY | | 4650000 | 3.26933E+05 | 3.20721E+10 |
| | | Nu | NUXY | | 0.397 | | |
| | | G | GXY | | 2270000 | 1.59599E+05 | 1.56567E+10 |
| | | dens | DENS | lb/cuin | 0.057 | 0.001603026 | 1577.781108 |
| | | ult ten | SIGXT | | 50000 | 3.51541E+03 | 3.44861E+08 |
| | | ult comp | SIGXC | | 38000 | 2.67171E+03 | 2.62095E+08 |
| | | sigyield | SIGYLD | | 44000 | 3.09356E+03 | 3.03478E+08 |
| | | | | | psi | kgf/cm/cm | N/m2 (Pascals) |

**Acknowledgements**

The author wishes to thank Dr. Dauglas Stanley, Georgia Institute of Technology, John Connolly, James R. Geffre, Johnson Space Center, Rudolph J. Soucillo, and Roger A. Lepsch, Langley Research Center, for the inspiration and partial funding during the Exploration Systems Architecture Study (ESAS) and Lunar Surface Access Module (LSAM) study. Additional funding was provided by Fay Collier, William Kimmel, and the Systems Analysis and Concepts Directorate.

**References**

1. NASA's Exploration Systems Architecture Study Final Report. NASA-TM-2005-214062, November 2005.
2. Griffin, Michael D., and French, James, R., "Space Vehicle Design," Second Edition, AIAA Publication, Reston, VA, 1991. (See also http://en.wikipedia.org/wiki/Apollo_Command/Service_Module.)
3. Mukhopadhyay, V., "Structural Configuration Analysis of Crew Exploration Vehicle Concepts," AIAA Paper 2006-2082, 47th AIAA/ASME Structures, Structural Dynamics and Materials Conf. Newport, RI, May 2006.
4. Mukhopadhyay, V., Sobieszczanski-Sobieski, J., Kosaka, I., Quinn, G., and Vanderplaats, G., "Analysis, Design and Optimization of Non-cylindrical Fuselage for Blended-Wing-Body Vehicle," *Journal of Aircraft*, Vol. 41, No. 4, *July-August, 2004, pp. 925-930.*
5. Glaessgen, E. H., Reeder, J. R., Sleight, D. W., Wang, J. T., Raju, I.S., Harris, C. E., "Debonding Failure of Sandwich Composite Cryogenic Fuel tank with Internal Core Pressure," Journal of Spacecraft and Rocket, Vol. 42, No. 4, July- August, 2005, pp. 613-627.
6. Aerospace Design Engineer's guide, 5th Edition. AIAA Publications, Reston, Virginia, September 2003.
7. SolidWorks User Manual, SolidWorks Corporation, Concord, Massachusetts.
8. CosmosM/CosmosDesignStar User manual, Structural Research and Analysis Corp. Los Angeles, California (http://www.cosmosm.com).
9. Greenberg, H. Stanley, "Structural Analysis techniques for preliminary Design of Launch vehicles," NASA Langley Short Course, Oct. 3-6, 2005.
10. Mukhopadhyay, V. S-Y Hsu, B. H. Mason, M. D. Hicks, W. T. Jones, D. W. Sleight, J. Chu, J. L. Spangler, H. Kamhawi, and J. L. Dahl, " Adaptive Modeling, Engineering Analysis and Design of Advanced Aerospace Vehicles," AIAA Paper 2006-2182, 47th AIAA/ASME Structures, Structural Dynamics, and Materials Conference, Newport, RI, May 2006.